Considerations limiting cyclotron-resonant damping of cascading interplanetary turbulence and why the 'slab' approximation fails

Robert J. Leamon,[1] William H. Matthaeus,[1] Charles W. Smith[1]
and
Hung K. Wong[2]

[1]*Bartol Research Institute, University of Delaware, Newark, DE*
[2]*Aurora Science Inc., San Antonio, TX*

Abstract. In attempting to understand the dissipation of MHD scale fluctuation energy in the solar wind, the challenge is to harness kinetic theory (1, 2) effects in a way that is consistent with the presence of an active spectral cascade in a collisionless plasma. Recent observational studies (3, 4) have begun the task of sorting out the constraints that spacecraft observations place on dissipation range dynamical processes. Here we examine some implications of inertial- and dissipation-range correlation and spectral analyses extracted from 33 intervals of WIND magnetic field data (4). When field polarity and signatures of cross helicity and magnetic helicity are examined most of the data sets suggest some role of resonant dissipative processes involving thermal protons. Here we seek an explanation for this effect by postulating that an active spectral cascade into the dissipation range is balanced by a combination of resonant and nonresonant kinetic dissipation mechanisms. By solving a pair of rate equations, and employing constraints from the data, this theory suggests that the ratio of the two methods of dissipation is of order unity. With an additional assumption that mixed cross helicity corresponds to random directional sweeping, the theory approximates the relationship between magnetic and cross helicities seen in the WIND datasets. Although highly simplified, this approach appears to account for several observed features, and explains why complete absorption, and the corresponding pure signature in the magnetic helicity spectrum, is usually not observed. The results of the theory are consistent with magnetic fluctuations having oblique wave vectors, which is strongly supported by the inability of models based on parallel-propagating waves to adequately predict the onset of the dissipation range.

INTRODUCTION

A number of presentations were made at the SW9 conference on the subject of collisionless heating, both in the solar corona and in the solar wind. The present paper employs *in situ* observations of magnetic dissipation that heats the solar wind to demonstrate the inconsistency between the prevailing "slab" model of parallel-propagating Alfvén waves and observations. As such, we constrain the nature of the magnetic fluctuations whose damping provides the *in situ* heating. In the process, we demonstrate the limitation of the popular ion cyclotron instability in the prediction of the onset of dissipation.

In this paper we again make use of the 33 one-hour intervals of magnetic field and plasma data recorded by the WIND spacecraft in near-Earth orbit first presented in Leamon *et al*. (4). Figure 1 shows the trace of the power spectral density matrix for Hour 13UT on January 30, 1995, which is typical in most regards of the collection of events used. At 0.44 Hz, the inertial range terminates in a sharp break to a steeper spectral index (the dissipation range). In all the events studied, this break frequency is comparable to, but always above, the proton cyclotron frequency (4, Figure 3).

The lower panel of Figure 1 shows the reduced magnetic helicity spectrum σ_m for that interval. Since σ_m is negative and $\langle B_R \rangle$ is also negative (the radial component of the field is directed inwards), this implies either a predominance of outward propagating, right-hand polarized waves or of inward propagating, left-hand polarized waves. We can determine which of these two possibilities is correct by comparing the normalized magnetic helicity spectrum σ_m in the dissipation range to the normalized cross helicity σ_c in the inertial range, which we do in Figure 2.

Magnetic helicity is a measure of the twist, or handedness of magnetic fields, and was first defined by

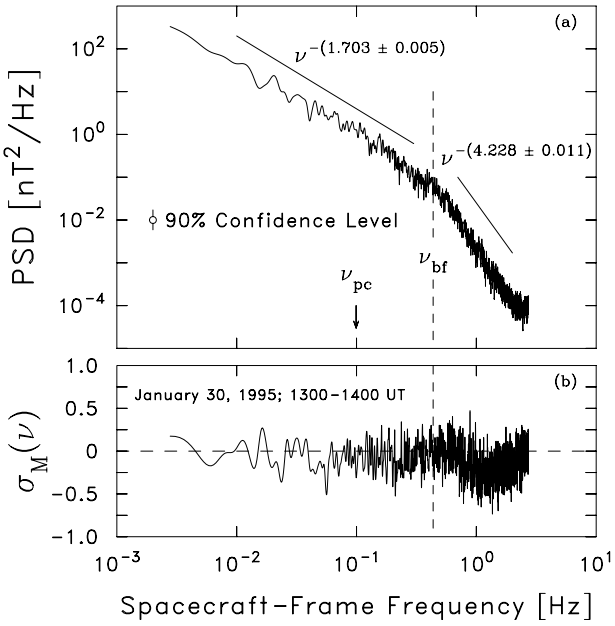

FIGURE 1. Typical interplanetary power spectrum showing the inertial and dissipation ranges. (a) Trace of the spectral matrix with a break at ~ 0.4 Hz where the dissipation sets in. (b) The corresponding magnetic helicity spectrum. For this period, $B = 6.4$ nT, $\beta_p = 0.71$, $V_{SW} = 692$ km s^{-1} and $\Theta_{BV} = 23°$. Reproduced from (4).

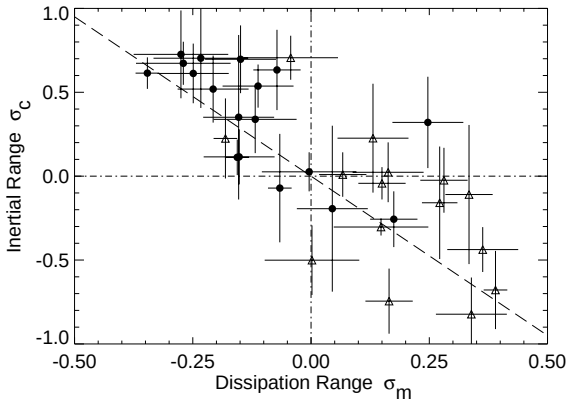

FIGURE 2. Scatter plot of the normalized cross-helicity in the inertial range, σ_c, vs. the normalized magnetic helicity in the dissipation range, σ_m. Triangles are intervals with outward directed mean magnetic field, and bullets have inwards mean fields. The dashed line corresponds to the best-fit line through the origin, $\sigma_c = -1.90\sigma_m$. Reproduced from (7).

Matthaeus and Golstein (5). Cross helicity can be defined in terms of the Elsässer energies (6). Both σ_c and σ_m are contrained to lie between -1 and $+1$.

The cross helicity can only be computed at inertial range frequencies because of limited sampling rates for plasma data; we use the inertial range σ_c as a proxy for the same quantity in the dissipation range. In effect, we are assuming that the direction of propagation of fluctuations is the same in both the inertial and dissipation ranges.

It is apparent from the data in Figure 2 that most intervals for which the mean magnetic field is outwardly directed have $\sigma_m > 0$ and $\sigma_c < 0$. On the other hand, inwards directed $\mathbf{B}_0$ is associated with $\sigma_m < 0$ and $\sigma_c > 0$. One can readily see that this is consistent with cyclotron-resonant absorption of outward-propagating fluctuations by thermal protons, as follows: A proton moving outward along the magnetic field executes a left-handed helical trajectory. Waves propagating outward at the Alfvén speed will overtake most thermal particles (at $\beta \approx 1$) and therefore, on average, the thermal protons will be in resonance with such waves that have a right-handed spatial structure ($\sigma_m < 0$). If the energy of these waves is assumed to be damped by the resonant protons, the energy that remains will preferentially reside in the undamped fluctuations, which have a left-handed structure and positive σ_m (8). Consequently, outward $\mathbf{B}_0$ should be associated with $\sigma_c < 0$ (outward propagation) and $\sigma_m > 0$. Reversing the direction of $\mathbf{B}_0$ but maintaining the assumption of outward propagating waves (now $\sigma_c > 0$) produces the conclusion that $\sigma_m < 0$ in the dissipation range by the same argument.

PARALLEL-PROPAGATING WAVES

Only 3 of the 33 intervals studied have helicity signatures that are inconsistent with cyclotron-resonant damping of Alfvén waves. This naturally suggests such resonant damping as a leading candidate for the formation of the dissipation range.

Recall that the resonance condition for cyclotron damping is

$$\omega - \mathbf{k}\cdot\mathbf{v} = \pm\Omega_p, \tag{1}$$

where $\mathbf{v}$ is the particle velocity. If we assume that the particles move with the thermal speed v_{th} and that damping sets in at $\omega = kv_A \ll \Omega_p$, equation 1 becomes $k_d = \Omega_p/(v_A + v_{th})$. Once we know the wavenumber at which dissipation starts, we may use the Doppler shift to conclude the frequency of an outward-propagating Alfvén wave resonant with a particle with the mean thermal speed:

$$\nu_{sc} = \frac{\mathbf{k}\cdot\mathbf{V}_{SW}}{2\pi} + \frac{\omega}{2\pi}. \tag{2}$$

Alternatively, we could argue that dissipation sets in at some critical wavenumber k_d where γ/ω (where ω

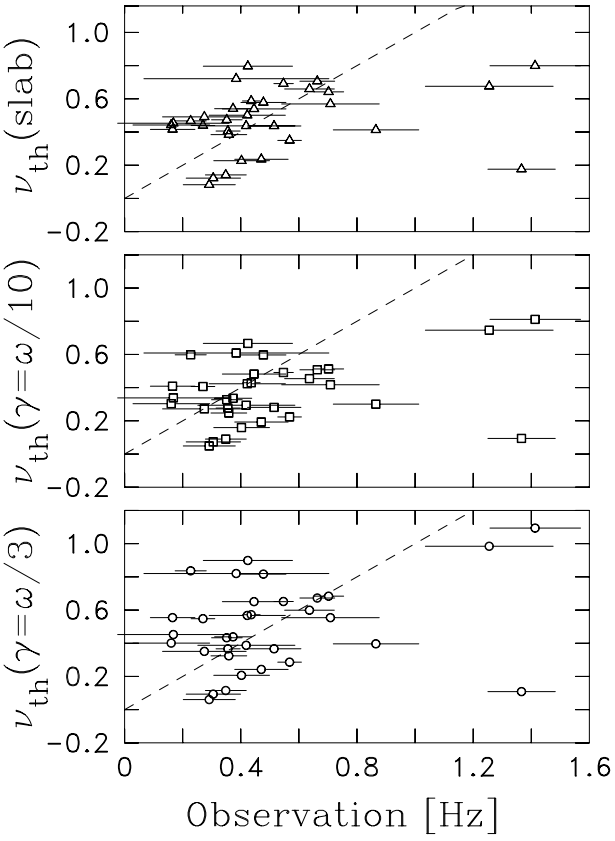

FIGURE 3. Comparison of observed spectral breakpoint frequency with predictions derived from the simple slab model (triangles, top panel) and the numerical results for $|\gamma| = \omega_r/10$ (squares, middle panel) and $|\gamma| = \omega_r/3$ (circles, bottom panel). Dashed lines represent equality. Although the predictions are generally in order-of-magnitude agreement with the observations, the necessary linear scaling is not observed. Reproduced from (4).

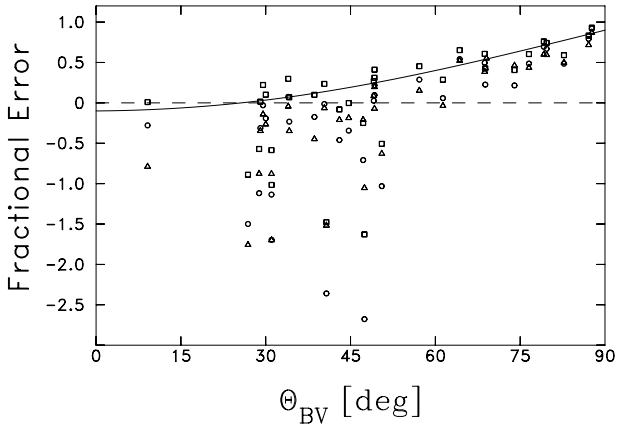

FIGURE 4. Fractional error for all three slab wave models discussed in the text as a function of field-to-flow angle Θ_{BV}. The symbols are the same as in Figure 3. The error is largest at large angles, true for all wave formulations. Reproduced from (4).

and γ are the real and imaginary parts of the wave frequency, respectively, calculated via solution of the linearized Vlasov-Maxwell equations) reaches some critical value, say one-third or one-tenth. We can again use equation 2 to Doppler-shift to a spacecraft-frame frequency.

Figure 3 compares the observed spectral break frequencies ν_{bf} with the predictions of our three cyclotron-resonance theories ν_{th}. All three models give order-of-magnitude agreement with the observations, but none exhibit any close correlation; the models are unsatisfactory. This might only reflect the simplicity of these three models were it not for an underlying order in the results not evident in this figure.

The systematic error of these theories is revealed in Figure 4, where we plot the fractional error of the theory relative to the observation, $(\nu_{bf} - \nu_{th})/\nu_{bf}$. Since we are assuming parallel-propagating Alfvén waves, the vector dot product in equation 2 implies a dependence on Θ_{BV} for the dissipation onset frequency for both the slab calculation and the numerical solutions. In fact, the break frequency ought to decrease by an order of magnitude as $\Theta_{BV} \rightarrow 90°$. (Since the solar wind speed V_{SW} is typically about 10 times faster than the Alfvén speed v_A, the first term on the RHS of equation 2 dominates the second except when $\Theta_{BV} \rightarrow 90°$.) However, the spectral break frequency remains almost constant and the percentage error increases to 100% as $\Theta_{BV} \rightarrow 90°$.

Any wave mode thought to be associated with the damping process and that propagates at less than the solar wind speed will suffer from a systematic introduction of error if the wave vector is required to be field-aligned. We must conclude, therefore, that the geometry of the fluctuations is not one-dimensional.

CASCADE AND DISSIPATION

While the exact nature of the oblique fluctuations is beyond the scope of this paper (see (4) and the following Leamon *et al.* paper in this volume), oblique wave fluctuations are generally susceptible to Landau damping (1).

Landau damping affects both right-hand and left-hand polarized fluctuations without regard for polarization, and thus affects the scatter of points in Figure 2, as we shall now show. The handedness argument used above explains the clustering of the observational points in the upper-left and lower-right quadrants. However, if kinetic processes are assumed to be very rapid, why is the signature in the magnetic helicity not pure (± 1) as one would expect for complete cyclotron absorption? We

must also include the contributions of Landau-resonant or completely nonresonant absorption, as well as relaxing the assumption of purely outward propagating fluctuations.

We can address these concerns by postulating a turbulent cascade and associated dissipation processes that are described by a pair of energy balance equations, as described in Leamon *et al*. (7) and summarised as follows:

$$\begin{aligned} \frac{dE_L}{dt} &= \frac{S}{2} - \gamma_0 E_L - P(L)\gamma_r E_L \\ \frac{dE_R}{dt} &= \frac{S}{2} - \gamma_0 E_R - P(R)\gamma_r E_R. \end{aligned} \quad (3)$$

The energies in left- and right-handed spatial structures, integrated over the dissipation range of the spectrum, are designated as E_L and E_R respectively. The rate of supply of energy (per unit mass) transferred into the dissipation range from the inertial range is designated by S. This supply rate is equally apportioned to L and R fluctuations since inertial range σ_m is random. The quantity γ_0 appears in both L and R equations and represents decay processes that produce no signature in the magnetic helicity. Included in γ_0 are contributions from Landau damping and other mechanisms that do not involve cyclotron resonance. The remaining damping term, γ_r, represents a decay rate due to cyclotron-resonant absorption by thermal protons. Its contribution needs to be apportioned to account for a distribution of propagation directions relative to the slower thermal protons. As such, $P(L)$ is the probability that fluctuations are propagating outward, which produces a resonance between left-handed structures and thermal protons, and implies the appearance of γ_r in the E_L equation. $P(R) = 1 - P(L)$ is the probability of inward propagation and implies that resonance between right-handed structures and thermal protons is weighted accordingly.

We can manipulate equations 3 to get a theoretical relationship between σ_c and σ_m to compare to Figure 2. Firstly, we assume that the cascade is steady, so that $dE_{L,R}/dt = 0$. E_L and E_R can be expressed in terms of σ_m. Assuming that outward propagation is proportional to the average outward-propagating energy, $P(L)$ may be written as $(1+\sigma_c)/2$. Finally, if we assume that γ_0 and γ_r are independent of σ_c and σ_m, we conclude

$$\sigma_c = -\left(1 + 2\frac{\gamma_0}{\gamma_r}\right)\sigma_m. \quad (4)$$

The best-fit line forced through the origin in Figure 2 is $\sigma_c = -1.90\sigma_m$. Putting this value into equation 4 implies that $\gamma_r = 2.22\gamma_0$. Only when $\gamma_0 = 0$ do pure Alfvén waves lead to purely helical states.

SUMMARY

This paper offers two complementary pieces of evidence against the prevailing idea that interplanetary turbulence is 'slab' waves.

The general ordering of the helicity data in Figure 2 suggests the dominant role of cyclotron-resonant damping. However, any model based on the damping of parallel-propagating Alfvén waves cannot predict the onset of the dissipation range, and therefore, the geometry of the fluctuations must be greater than one-dimensonal.

Oblique waves are susceptible to both cyclotron and Landau damping. Using our cascade-and-dissipation model outlined above, we can demonstrate the oblique nature of IMF fluctuations via the inferred presence of Landau damping. Our model is highly simplified and idealised; nevertheless, it explains the finer details of Figure 2, by requiring that on average, about one-third of the damping comes from such processes as Landau damping.

This work is supported by NASA grants NAG5-3026 and NAG5-7164, NASA subcontract NAG5-2848, and NSF grant ATM-9713595 to the Bartol Research Institute. The participation of H.K.W. is supported by NASA contract NAS5-32484 and by a grant to the Goddard Space Flight Center from the NASA Space Physics Theory Program.

REFERENCES

1. Barnes, A., in *Solar System Plasma Physics*, **1**, edited by E. N. Parker, C. F. Kennel, and L. J. Lanzerotti, 249–319, New York: North-Holland (1979).
2. Montgomery, D. C., *J. Geophys. Res.*, **97**, 4309–4310 (1992).
3. Goldstein, M. L., D. A. Roberts, and C. A. Fitch, *J. Geophys. Res.*, **99**, 11 519–11 538 (1994).
4. Leamon, R. J., C. W. Smith, N. F. Ness, W. H. Matthaeus, and H. K. Wong, *J. Geophys. Res.*, **103**, 4775–4787 (1998).
5. Matthaeus, W. H., and M. L. Goldstein, *J. Geophys. Res.*, **87**, 6011–6028 (1982).
6. Marsch, E., and A. Mangeney, *J. Geophys. Res.*, **92**, 7363–7367 (1987).
7. Leamon, R. J., W. H. Matthaeus, C. W. Smith, and H. K. Wong, *Astrophys. J. Lett.*, **507**, L181–L184 (1998).
8. Moffatt, H. K., *Magnetic Field Generation in Electrically Conducting Fluids*, New York: Cambridge University Press (1978).